



Contents lists available at ScienceDirect

Chemical Geology

journal homepage: www.elsevier.com/locate/chemgeo

Tracing the sources of cave sulfates: a unique case from Cerna Valley, Romania

Bogdan P. Onac^{a,b,*}, Jonathan G. Wynn^a, Jonathan B. Sumrall^c^a Department of Geology, University of South Florida, 4202 E. Fowler Ave., SCA 528, Tampa, FL 33620, USA^b Department of Geology, "Babeş-Bolyai" University, Cluj/"Emil Racoviţă" Institute of Speleology, Clinicilor 5, 400006 Cluj, Romania^c Department of Geosciences, Mississippi State University, P.O. Drawer 5448, Mississippi State, MS 39762, USA

ARTICLE INFO

Article history:

Received 21 October 2010

Received in revised form 5 July 2011

Accepted 11 July 2011

Available online 23 July 2011

Editor: U. Brand

Keywords:

Sulfur isotopes

Cave sulfates

Thermo-mineral springs

Sulfuric acid speleogenesis

ABSTRACT

In order to reliably distinguish between different genetic processes of cave sulfate formation and to quantify the role of thermo-mineral waters on mineral deposition and cave morphology, it is critical to understand sulfur (S) sources and S transformations during hydrological and speleogenetic processes. Previous work has shown that sulfuric acid speleogenesis (SAS) often produces sulfate deposits with ^{34}S -depleted isotopic signatures compared to those of the original source of S in sulfate rocks. However, ^{34}S -depleted isotopic composition of S-bearing minerals alone does not provide enough information to clearly distinguish SAS from other speleogenetic processes driven by carbonic acid, geothermal heat, or other processes. The isotopic composition ($\delta^{18}\text{O}$ and $\delta^{34}\text{S}$) of sulfate minerals (mainly gypsum) from seven caves of the Cerna Valley (Romania) defines three distinct populations, and demonstrates that the $\delta^{34}\text{S}$ values of SAS-precipitated cave sulfates depend not only on the source of the S, but also on the $\text{H}_2\text{S}:\text{SO}_4^{2-}$ ratio during aqueous S species reactions and mineral precipitation. Population 1 includes sulfates that are characterized by relatively low $\delta^{34}\text{S}$ values (-19.4 to -27.9‰) with $\delta^{18}\text{O}$ values between 0.2 and 4.3‰ that are consistent with oxidation of dissolved sulfide produced during methane-limited thermochemical sulfate reduction (TSR) that presently characterizes the chemistry of springs in the upper Cerna Valley. Population 2 of cave sulfates has ^{34}S -enriched $\delta^{34}\text{S}$ values (14.3 to 19.4‰) and more ^{18}O -depleted $\delta^{18}\text{O}$ values (from -1.8 to -10.0‰). These values argue for oxidation of dissolved sulfide produced during sulfate-limited TSR that presently characterizes the chemistry of springs further downstream in the Cerna Valley. The $\delta^{18}\text{O}$ values of cave sulfates from Population 1 are consistent with oxidation under more oxic aqueous conditions than those of Population 2. $\delta^{34}\text{S}$ values of cave sulfates within Population 3 ($\delta^{34}\text{S}$: 5.8 to 6.5‰) may be consistent with several scenarios (*i.e.*, pyrite oxidation, oxidation of dissolved sulfide produced during methane-limited TSR coupled with O_2 -limited oxidation during SAS). However, comparatively ^{18}O -enriched $\delta^{18}\text{O}_{\text{SO}_4}$ values (11.9 to 13.9‰) suggest the majority of this sulfate O was derived from atmospheric O_2 in gas-phase oxidation prior to hydration. Thus, the combined use of oxygen- and sulfur-isotope systematics of sulfate minerals precipitated in a variety of cave settings along Cerna Valley may serve as an example of how more complex cave systems can be deconvoluted to allow for more complete recognition of the range of processes and parameters that may be involved in SAS.

Published by Elsevier B.V.

1. Introduction

Although sulfates are the second most important group of cave minerals, and gypsum is the second most abundant cave mineral after calcite (Onac, 2005), the sources of sulfur (S) in limestone caves are often poorly understood. Sulfur in cave minerals is thought to derive from one of four sources: oxidation of sulfides, dissolution of evaporites in interbedded or overlying limestone, decomposition of bat guano, and from postvolcanic activities (Hill and Forti, 1997). Discriminating between these sources may be aided by studies of S

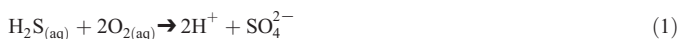
isotopic composition because large isotope fractionation occurs in many biogeochemical reactions between reduced and oxidized species, and causes sulfur isotopic composition to vary by as much as 180‰ in various geological materials (Hoefs, 2009; analytical precision is $< \sim 0.5\text{‰}$). Therefore, S isotope analyses can be used for different applications within hydrology, ore deposits, sedimentary geology, environmental studies, *etc.*, with the target being to obtain information on the source of S, as well as biogeochemical reaction progress and redox conditions (Ohmoto, 1972; Seal et al., 2000; Canfield, 2004; Bottrell and Newton, 2006; Ono, 2008; Mandeville, 2010). Over 400 publications investigating the mineralogy of sulfates in caves have been published (for a complete list see Hill and Forti, 1997; Onac and Forti, 2011), but only a few studies have used stable isotope analysis to trace the origin of S in cave sulfates (van Everdingen et al., 1985; Hill, 1987, 1990, 1995; Yonge and Krouse,

* Corresponding author at: Department of Geology, University of South Florida, 4202 E. Fowler Ave., SCA 528, Tampa, FL 33620, USA. Tel.: +1 813 974 1067; fax: +1 813 974 2654.

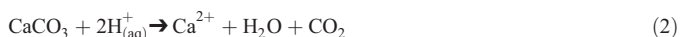
E-mail addresses: bonac@usf.edu (B.P. Onac), wynnj@usf.edu (J.G. Wynn), jbs105@gmail.com (J.B. Sumrall).

1987; Bottrell, 1991; Bottrell et al., 1993, 2001; Swezey et al., 2004; Lueth et al., 2005; Onac et al., 2007, 2009). Fewer have combined S isotopes with information to be gained from O isotopic composition (van Everdingen et al., 1985; Grasby et al., 2003).

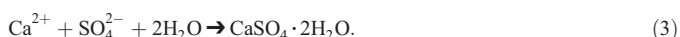
Abundant gypsum deposits, combined with particular passage morphologies (e.g., cupolas, irregular rooms, floor feeders – i.e., inlets for deep-seated fluids, etc.) have prompted scientists to suggest a new model of speleogenesis that is an alternative to the classical limestone dissolution model in which CO₂ is the source of acidity (Jagnow et al., 2000; Palmer and Hill, 2005; Palmer, 2007). Morehouse (1968) was first to suggest sulfuric acid speleogenesis (SAS) by pyrite oxidation in some small cavities in Iowa. Shortly after, Egemeier (1973), based on his work in the Kane Caves (Wyoming) proposed a new SAS model entirely based on chemical oxidation of H₂S to sulfuric acid. This model was later recognized and shown to be an important process in the development of some major cave systems (e.g., Carlsbad Caverns, Lechuguilla, Villa Luz, Frasassi, Movile, etc.; Jagnow, 1977; Hill, 1981, 1987; Pisarowicz, 1994; Galdenzi and Menichetti, 1995; Sarbu et al., 1996; Polyak et al., 1998). The SAS model was fundamentally refined when the microbial contribution to the H₂S oxidation to sulfuric acid by subaqueous sulfur-oxidizing bacteria was documented by Angert et al. (1998), Hose et al. (2000), Vlasceanu et al. (2000), and especially Engel et al. (2004). Thus, the SAS biotic-pathway is now considered a key mechanism responsible for subaqueous aggressive dissolution of limestone bedrock, gypsum replacement of carbonate surfaces, and subaerial precipitation of extensive gypsum deposits (Engel et al., 2004; Barton and Northup, 2007). The oxidation of dissolved sulfide takes place according to the following reaction (Canfield, 2001; Rye, 2005; Palmer, 2007):



Total dissolved sulfide (H₂S, HS[−] and S^{2−}) is simply denoted in this reaction as H₂S_(aq); also the chemistry of the reaction is not as simple as this reaction stoichiometry implies, but instead the oxidation of sulfide actually passes through several intermediates of different oxidation states (Zhang and Millero, 1994). The acid generated by this oxidation corrodes cave limestone to liberate Ca²⁺,



which may then precipitate gypsum:



SAS is now recognized in caves in the United States, Italy, Mexico, Canada, Romania, and France. A complete review of the history of sulfuric acid theory of speleogenesis (including sources of sulfide) is supplied by Jagnow et al. (2000), Palmer and Hill (2005), and references cited therein.

This research aims to document the potential S sources of sulfates in the caves of the Cerna Valley and further emphasize that SAS is, and was an active cave-forming process in this region. We describe the occurrence and distribution of sulfates from seven caves and relate cave minerals to dissolved S species from the thermo-mineral springs near Băile Herculane, Romania. The implications of this study are not restricted to the karst and cave environment. For instance, some SAS by-products (e.g., alunite) can be dated by K/Ar or Ar/Ar methods constraining timing of SAS (Polyak et al., 1998). In turn, such information can contribute to our understanding on the local tectonic processes, such as the incision of the Danube Gorge, and more importantly, in predicting regional groundwater dynamics and migration patterns of thermal activity that may impact the historic spas of Băile Herculane.

2. Geological and hydrogeological settings

Băile Herculane, in the Cerna Valley of southwestern Romania (Fig. 1), is a unique resort city that has exploited local thermo-mineral waters for their balneotherapeutic qualities since before the arrival of the Romans (A.D. 107; Cristescu, 1978; Povară, 2001). The presence of these thermo-mineral waters with temperatures ranging between 9.8 and 60 °C is related to an intruded granitoid body, which triggered a positive geothermal anomaly, with thermal gradients six fold higher than the regional average, identified in the lower part of the Cerna Valley (Gheorghe and Crăciun, 1993; Demetrescu and Andreescu, 1994; Veliciu, 1998; Povară et al., 2008).

The basement of the Cerna Valley (Danubian nappes) consists of fractured Precambrian high-grade, partly migmatitic series, intruded by granitoids of Panafrican age (Liégeois et al., 1996; Iancu et al., 2005). Locally this basement is covered by Permian redbeds, followed by a transgressive sequence of Lower Jurassic conglomerates, sandstones, and white arkoses (Gresten facies). The transgressive sequence is overlain by Middle Jurassic sandstones with carbonatic matrix and Late Jurassic to Early Cretaceous massive platform limestones that host most of the Cerna Valley caves. The Early Cretaceous sedimentary sequence ends with a 200–250 m thick compact or schistose marly limestone known as Iuta Layers (Năstăseanu, 1980; Bercia et al., 1987).

Along the Cerna Valley two distinct thermo-mineral aquifer complexes develop. The Northern Aquifer stretches over ~20 km, between Bobot Gorges to the north and the Granite Sill to the south (Fig. 1). The springs emerging from this aquifer are typical karst carbonate waters (pH between 6.2 and 8.6) with very low (<0.03) ionic strength (Marin, 1984). The total dissolved solids (TDS) rarely exceed 300 mg/L whereas the average sulfate concentration is ~9 mg/L. The temperatures of the waters discharging from the Northern Aquifer increase from 9.8 °C in the north to about 34 °C at the southern limit of the aquifer. The Southern Aquifer extends for ~5 km downstream from Aburi Cave. The subsurface thermal waters (T from well waters ranges between 38 and 60 °C; pH from 5.1 to 7.8) are ascending from depth along transversal fractures or karst voids. The ionic strength of the alkali-chloride- and sulfurous-type waters is between 0.1 and 0.22. Sulfate concentrations vary from 15 to 115 mg/L and the TDS approximately to 4500 mg/L (Wynn et al., 2010; Marin, unpubl. data).

Downstream of Băile Herculane, the mineralization of the Cerna River waters is higher (average values in mg/L; TDS: 175; SO₄^{2−}: 15.7; Ca²⁺: 30.5; Na⁺+K⁺: 14.5; HCO₃[−]: 87.7; Cl[−]: 20.7; Mg²⁺: 3.0) compared to its upstream section (average values in mg/L; TDS: 76; SO₄^{2−}: 6.1; Ca²⁺: 14.5; Na⁺+K⁺: 1.8; HCO₃[−]: 50.2; Cl[−]: 1.2; Mg²⁺: 1.3) (Marin, 1984). This is due to the discharge of thermo-mineral sources in the area around the Băile Herculane Spa. However, the Cerna waters are undersaturated with respect to calcite and gypsum along the entire flow path. The average temperature of waters in the Cerna River is 11.7 °C.

3. Cave passages morphology and mineral precipitation

The caves in the Cerna Valley are either epigenic (formed from carbonic acid dissolution at or near the surface), hypogenic (formed via SAS), or polygenic. The majority of caves adjacent to Băile Herculane (later referred to as the “caves downstream in Cerna Valley”) show morphological features indicative of SAS origin, such as ceiling pockets, ascending blind passages, and floor feeders (Klimchouk, 2007; Palmer, 2007), whereas in the upper Cerna Valley evidence indicates polygenic caves (e.g., Sălitari and Bîrzeni caves). These morphological features, along with some minerals considered primary speleogenetic by-products (DuChene, 1997; Polyak and Provencio, 2001; Palmer and Hill, 2005; Audra et al., 2007; Onac et al., 2007) provide unequivocal evidence that dissolution of limestone by sulfuric acid may have played a significant role in the speleogenesis of at least some of the caves within this karst region.

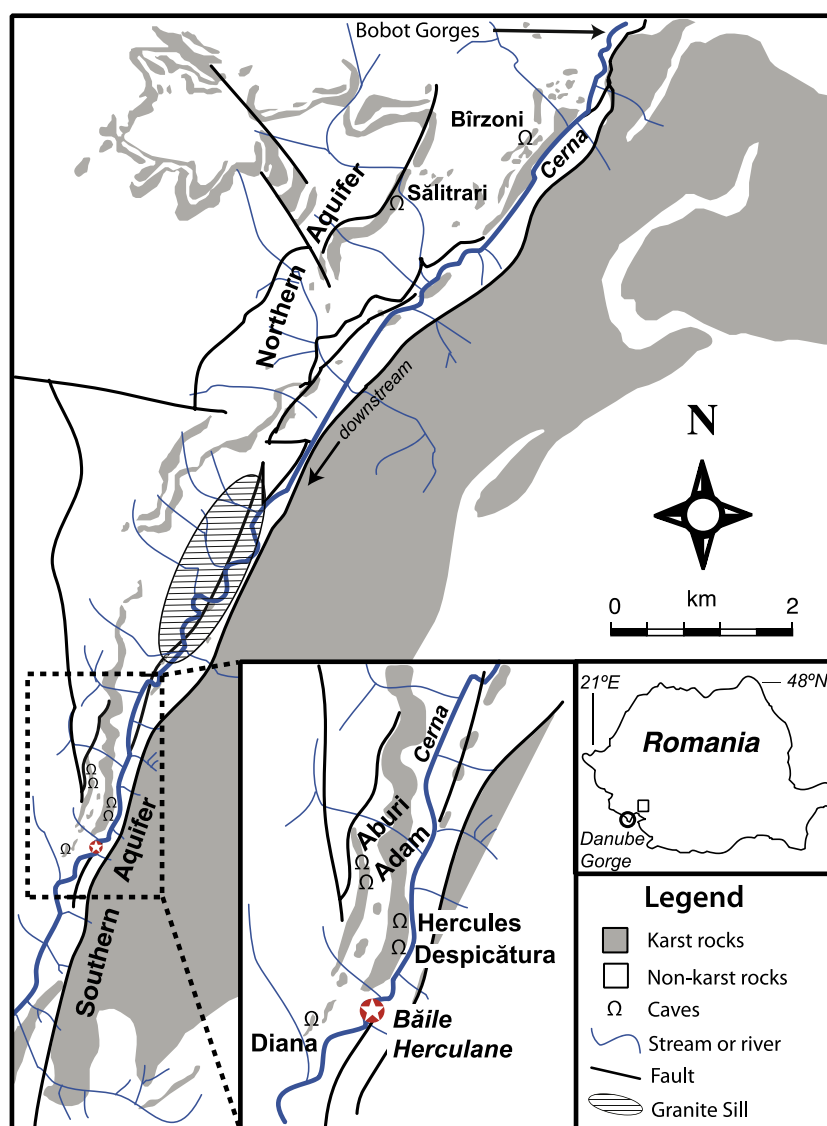


Fig. 1. Location of study area showing cave locations with respect to karst and non-karst rocks.

Sălitrari and Bîrzeni caves are located north of Băile Herculeane in the upstream section of the Cerna Valley (Fig. 1). They consist of old fossil passages with no active stream conduits or hot steam emissions, but only meteoric waters dripping or seeping from the roof. Both caves are highly decorated with vadose calcite speleothems (*i.e.*, stalactites, stalagmites, crusts, flowstones, *etc.*). Although gypsum crusts are widespread in these two caves, the only perceptible precipitation process is that of calcite.

The caves downstream in Cerna Valley (Fig. 1 inset) were divided by Povară et al. (1972) into two groups: 1) caves in which H_2S -rich thermo-mineral waters discharge (*e.g.*, Diana, Despicătură, and Hercules) and 2) caves with H_2S -rich steam (up to 52 °C) emissions (*e.g.*, Aburi and Adam).

Notable for the first group is that the thermal waters (up to 53.2 °C) either pool or flow along cave passages reacting with the limestone or other interbedded rocks (marls, shales) to precipitate gypsum or other sulfate minerals in the form of aggregates and wall crusts (Povară et al., 1972; Onac et al., 2009). In addition, efflorescences of gypsum, tamarugite, and hallotrichite-group minerals are the main products of the bedrock alteration by acid sulfate condensate generated above the pools or thermal waters flow paths. These caves provide a

sheltered, climatically stable micro-environment in which the alteration processes of steam condensate upon limestone or other exposed rocks causes unusual SAS Al-rich by-products to form and persist. Despicătură Cave, however, is an exception; the two thermal springs naturally discharging in the cave were captured and diverted to a nearby hotel for balneotherapeutic use. Despicătură Cave hosts the largest gypsum deposits (crusts and blocky aggregates) among any of the downstream Cerna caves. In all three caves of this group, minerals are also precipitated subaqueously (however, for this study, we only collected presently subaerial samples).

Small fumaroles are typical in the floors for the second group of caves (~0.3 to 0.5 m in diameter). Around these vents, thin (<0.5 mm) microcrystalline gypsum crusts are actively forming. Calcite is also forming in Aburi and Adam caves from seeping meteoric water. Furthermore, phosphate minerals (related to the presence of large amounts of bat guano) were documented in the Adam Shaft (Onac et al., 2009).

The air temperature in the caves downstream in Cerna Valley varies between 23 and 45 °C, whereas the relative humidity is in the range of 97 to 100%. In contrast to the caves upstream in Cerna Valley, sulfurous gasses are acutely evident in all caves near Băile Herculeane Spa.

4. Previous work on sulfuric acid speleogenesis using sulfur isotopes

To document the source of the large gypsum deposits of Carlsbad Caverns, Lechuguilla, and other caves in the Guadalupe Mountains, stable isotopic analysis has provided some of the most robust evidence. Several studies in these caves identified gypsum with low $\delta^{34}\text{S}$ values ($\delta^{34}\text{S} = -25.6\text{‰}$), and attributed these values to H_2S produced by microbial dissimilatory sulfate reduction, with abundant sulfate derived from minerals in the Castile Formation (initial $\delta^{34}\text{S}$ of sulfate $\sim +10\text{‰}$; $\delta^{34}\text{S}$ of sulfide $\sim -20\text{‰}$) and electrons being provided by hydrocarbon deposits of the Delaware Basin (Hill, 1987, 1990; Spirakis and Cunningham, 1992). Because dissimilatory sulfate reduction here is limited by electron supply, a large fractionation factor is evident between sulfate and sulfide ($\Delta_{\text{SO}_4-\text{H}_2\text{S}} \sim 30\text{‰}$). These waters, charged with relatively ^{34}S -depleted H_2S , ultimately ascend to mix with surficial-derived oxalic freshwater. The sulfuric acid responsible for limestone replacement, gypsum deposition, and cave enlargement was generated as this mixing occurred (Reaction 1). If the oxidation of H_2S happens in a closed system (i.e., no H_2S escapes), the sulfur isotopic composition of the sulfuric acid produced must reflect the isotopic composition of H_2S from which it is produced. And, if the oxidation is nearly complete (low $\text{H}_2\text{S}:\text{SO}_4^{2-}$), little or no fractionation is evident between reactants and products and thus, the initially low $\delta^{34}\text{S}$ values of the ascending sulfide are retained.

Studies of Frasassi caves in central Italy also showed that these caves were also formed via sulfuric acid dissolution. Hydrogen sulfide is generated by microbial dissimilatory sulfate reduction, with sulfate likely derived from anhydrite. This process happens in the underlying Triassic limestones that also contain abundant organic C, providing electron donors for microbial dissimilatory sulfate reduction (Galdenzi and Menichetti, 1995). As the H_2S generated later ascends through the more oxic groundwater, it is partially oxidized to sulfuric acid by sulfur-oxidizing bacteria (Macalady et al., 2006). Some of the H_2S gas also diffuses into the more oxic cave atmosphere, where it may be more completely oxidized by O_2 to sulfuric acid in surficial condensates. The acid reacts with limestone, which is then replaced with gypsum that shows $\delta^{34}\text{S}$ values more depleted than the mineral source ($\delta^{34}\text{S}$ from -19 to -6‰), thus reflecting the S isotopic composition of the dissolved sulfide. Minor $\delta^{34}\text{S}$ variation may be due to variation in the degree of microbial oxidation or potentially during a second stage of bacterial sulfate reduction within the cave (Galdenzi and Menichetti, 1995; Galdenzi and Maruoka, 2003).

Sulfur isotopic composition of gypsum ($\delta^{34}\text{S} \sim -23\text{‰}$) in Villa Luz Cave (Mexico) is comparable to those in the Guadalupe Mountains (Spirakis and Cunningham, 1992). However, the yet unconfirmed source of H_2S is considered to be the bacterial reduction of evaporite sediments using hydrocarbons from the nearby oil fields as the source of electron donors (Hose et al., 2000).

Oxidation of sulfides (e.g., pyrite and marcasite) is another mechanism that ultimately generates sulfuric acid solutions, such as in acid mine drainage (Taylor and Wheeler, 1994; Haubrich and Tichomirowa, 2002). However, by itself, this process alone is not known to be responsible for producing any major cave passages. As fractionation factors involved in this process are generally very small, the expected isotopic composition of sulfate produced by this mechanism should ultimately track that of the source sulfide minerals.

It can be generalized from the above discussion and other studies that S isotope fractionation during S oxidation is comparatively small (nil fractionation at high T, see Schoen and Rye, 1970; Ohmoto, 1972; Ohmoto and Rye, 1979; Taylor and Wheeler, 1994; small fractionation at low T, see Kaplan and Rittenberg, 1964; Fry et al., 1988). Hence the S isotopic composition of oxidized SAS by-products (e.g., gypsum, Al-sulfates) allows tracing the S pathway up to the formation of sulfuric acid (Yonge and Krouse, 1987; Bottrell, 1991; Bottrell et al., 1993, 2001). Because minerals produced via the SAS pathway undergo

little isotopic fractionation between sulfide and sulfate, they will reflect the original isotopic composition of the source of reduced S.

5. Materials and methodology

Onac et al. (2009) investigated 13 caves of the Cerna region and found 22 minerals, including 16 minerals that had not previously been identified in the region. Additional mineralogical information on the Great Săitrari Cave was reported by Pușcaș et al. (2010). The most common sulfate mineral was gypsum (sampled as crusts from all investigated caves), and the most exotic mineral assemblages were documented in Diana and the Great Săitrari caves. For this study, we sampled S-bearing cave minerals from a total of seven caves (locations shown in Fig. 1) with 37 samples total. These samples included sulfates (gypsum, $\text{CaSO}_4 \cdot 2\text{H}_2\text{O}$; alunite, $\text{KAl}_3(\text{SO}_4)_2(\text{OH})_6$; aluminite, $\text{Al}_2\text{SO}_4(\text{OH})_4 \cdot 7\text{H}_2\text{O}$; and tamarugite, $\text{NaAl}(\text{SO}_4)_2 \cdot 6\text{H}_2\text{O}$) and one hydrous nitrate and sulfate of sodium [darapskite; $\text{Na}_3(\text{SO}_4)(\text{NO}_3) \cdot \text{H}_2\text{O}$] in the form of crusts, efflorescent masses, aggregates, and anhydrous crystals (see Table 1 for details). In addition, three grains of diagenetic pyrite (confirmed by X-ray powder diffraction analyses) were recovered from the limestone bedrock that hosts Bîrzoni Cave. The pyrite grains (less than 0.7 mm across) consist of subhedral crystals with cubo-pyritohedral morphologies.

An Isotope Ratio Mass Spectrometer (IRMS; [Delta V; ThermoFinnigan, Bremen]) at the University of South Florida Stable Isotope Lab was used to measure $^{34}\text{S}/^{32}\text{S}$ ratio of S-bearing minerals. Results are reported in delta (δ)-notation with respect to the Cañon Diablo

Troilite (CDT) standard, where: $\delta^{34}\text{S}_{\text{sample-CDT}} = \left[\left(\frac{^{34}\text{S}/^{32}\text{S}}{^{34}\text{S}/^{32}\text{S}} \right)_{\text{sample}} / \left(\frac{^{34}\text{S}/^{32}\text{S}}{^{34}\text{S}/^{32}\text{S}} \right)_{\text{CDT}} - 1 \right] 1000\text{‰}$.

Isotope ratios were measured by coupled Elemental Analysis EA-IRMS ([Costech ECS 4100, Milano]); Grassineau et al., 2001). The results were normalized to CDT using $\delta^{34}\text{S}$ values of the four IAEA standards (IAEA, International Atomic Energy Agency, S-2, $\delta^{34}\text{S} = 22.7\text{‰}$ and IAEA S-3, $\delta^{34}\text{S} = -32.3\text{‰}$, for sulfides and IAEA SO-5, $\delta^{34}\text{S} = 0.5\text{‰}$, and IAEA SO-6, $\delta^{34}\text{S} = -34.1\text{‰}$ for sulfates). The reproducibility between replicate standards in each run was estimated to be better than $\pm 0.1\text{‰}$ (1σ). An IRMS at the Environmental Isotope Laboratory (University of Arizona) was used to measure the isotopic composition of oxygen in the sulfate site of all sulfate-bearing minerals. Results are reported in delta (δ)-notation with respect to the Vienna Standard Mean Ocean Water (VSMOW) standard, where $\delta^{18}\text{O}_{\text{sample-VSMOW}} =$

$\left[\left(\frac{^{18}\text{O}/^{16}\text{O}}{^{18}\text{O}/^{16}\text{O}} \right)_{\text{sample}} / \left(\frac{^{18}\text{O}/^{16}\text{O}}{^{18}\text{O}/^{16}\text{O}} \right)_{\text{VSMOW}} - 1 \right] 1000\text{‰}$. Isotope ratios were measured on CO gas in a continuous-flow IRMS (ThermoQuest Finnigan Delta PlusXL; Nehring et al., 1977). Samples were combusted with excess C at 1350°C using a thermal combustion elemental analyzer (ThermoQuest TC/EA) coupled to the IRMS. Standardization is based on the international standard OGS-1, with a recommended $\delta^{18}\text{O}$ value of 9.2‰ . Precision is estimated to be $\pm 0.7\text{‰}$ or better (1σ), based on replicate internal standards in each run.

6. Results and discussion

The isotopic composition ($\delta^{18}\text{O}$ and $\delta^{34}\text{S}$) of sulfates and sulfides from the investigated caves is listed in Table 1. Plotted in Fig. 2, the data show three distinct populations with significant variations between them, but relatively homogeneous within each cave location. Population 1 includes gypsum crusts from Bîrzoni Cave and the inner portion of Săitrari Cave that are characterized by relatively low $\delta^{34}\text{S}$ values (-19.4‰ to -27.9‰) with $\delta^{18}\text{O}$ values between 0.2 and 4.3‰. Population 2 includes samples of gypsum and tamarugite crusts and efflorescent masses from Hercules, Despicătura, and Diana caves, which are located in the Băile Herculane Spa, and have ^{34}S -enriched

Table 1
Sulfur and oxygen isotope values of cave sulfate minerals.

Cave	Sample no.	GPS location	$\delta^{34}\text{S}$ (‰)	$\delta^{18}\text{O}$ (‰)	Occurrence	Mineral	Mineral habit
Birzoni	1699	^a	−27.2	2.0	Crust	Gypsum	Granular
	1700		−26.4	3.7	Crust	Gypsum	Granular
	1701		−26.3	1.7	Crust	Gypsum	Granular
	1702		−27.7	1.5	Crust	Gypsum	Granular
	1703a		−27.5	0.9	Crust	Gypsum	Granular
	1703b		−27.4	1.2	Crust	Gypsum	Granular
	1704		−27.9	0.2	Crust	Gypsum	Granular
	1705		−23.0	4.3	Crust	Gypsum	Granular
	PB-1		9.4	–	Disseminated	Pyrite	Disseminated
	PB-2		7.9	–	Disseminated	Pyrite	Disseminated
Diana	PB-3		7.1	–	Disseminated	Pyrite	Disseminated
	1770	N44°53,367'	19.4	−8.9	Efflorescence	Tamarugite	Fibrous/acellular
	1771	E22°25,414'	18.0	−9.1	Efflorescence	Tamarugite	Fibrous/acellular
	1772		18.6	−9.2	Efflorescence	Gypsum	Fibrous/acellular
	1773		19.1	−9.1	Efflorescence	Gypsum	Fibrous/acellular
	1774		19.3	−10.0	Crust	Gypsum	Granular
	1775		19.5	−9.7	Crust	Gypsum	Granular
	1776		19.2	−7.8	Crust	Gypsum	Granular
	1777		18.8	−9.4	Efflorescence	Gypsum	Efflorescence
Despicătură	1779	N44°53,684'	18.5	−6.0	Crust	Gypsum	Granular
	1782	E22°25,690'	17.0	−5.6	Crust	Gypsum	Granular
	1783		17.6	−5.8	Crust	Gypsum	Granular
	1784		14.3	−5.9	Crust	Gypsum	Granular
Hercules	1787	N44°53,670'	14.1	−1.8	Crust	Gypsum	Granular
	1787a	E22°25,697'	13.7	−2.6	Crust	Gypsum	Granular
Great Săitrari (inner part)	1788	^a	−19.8	4.2	Crust	Gypsum	Granular
	1789		−22.4	4.0	Crust	Gypsum	Granular
	1790		−21.6	4.3	Crust	Gypsum	Granular
	1792		−21.1	3.9	Crust	Gypsum	Granular
Great Săitrari (Nitrate Passage)	1799a	^a	6.5	13.9	Crystal	Darapskite	Acicular
	1799b		5.6	13.4	Aggregate	Alunite	Tabular
	1801		5.9	13.1	Aggregate	Aluminite	Earthy
	1802a		5.7	13.3	Crusts	Gypsum	Granular
Aburi	1806	44°53,907'	6.5	12.9	Crust	Gypsum	Granular
	1807	22°25,618'	5.8	12.4	Crust	Gypsum	Granular
Adam	1811	44°53,849'	6.5	12.7	Crust	Gypsum	Granular
	1812	22°25,648'	6.3	11.9	Crust	Gypsum	Granular

^a The precise location is not specified in order to protect these caves from potential vandalism.

$\delta^{34}\text{S}$ values (14.3 to 19.4‰), whereas the $\delta^{18}\text{O}$ values range from −1.8 to −10.0‰. Within this group of three caves, the isotopic composition of sulfates progressively becomes more ^{18}O -enriched and ^{34}S -depleted in a downstream direction towards Diana Cave (Fig. 2). Population 3 includes sulfates (and one nitrate) from Aburi Cave, the Nitrate Passage of Săitrari Cave, and Adam Shaft (Table 1) and is characterized by high $\delta^{18}\text{O}$ values (11.9 to 13.9‰) and moderately high $\delta^{34}\text{S}$ values (5.8 to 6.5‰).

To ascertain the cause of stable isotopic variations seen between the three populations, we utilize a dual isotopic approach of S and O in sulfates, and discuss the compositions of both elements separately below. Sulfur isotopic composition provides information on the source and reaction pathway of S involved in the initial stage of sulfate reduction (either by biotic or abiotic), but very little information on the secondary processes of oxidation during SAS. Oxygen isotopic composition of sulfate provides information of the source and reaction pathway of O involved in this secondary stage of oxidation of sulfides, independent of information gained on origin of S in sulfides.

6.1. S-isotope evolution during TSR and preservation of $\delta^{34}\text{S}$ values during subsequent SAS

Sulfur isotopic composition of sulfate mineral Populations 1 and 2 partly overlap with those of dissolved S in the two karst aquifers, each of which have distinct water chemistries and $\delta^{34}\text{S}$ values (Fig. 2). We directly relate these S isotopic compositions to the water chemistry of the two Cerna aquifers. Wynn et al. (2010) described the unique set of

conditions in the aquifers of the Cerna region, which allow the various stages of methane-mediated thermochemical sulfate reduction (TSR) to be expressed in the springs and wells surrounding Băile Herculane Spa. Using this study of dissolved sulfur species, we apply a model from Ohmoto and Rye (1979) that predicts $\delta^{34}\text{S}$ evolution during sulfur reduction (TSR) and oxidation (SAS) stages in a system that is closed with respect to sulfate. In Fig. 3, we show this model, using values of initial $\delta^{34}\text{S}$ of sulfate and the isotope enrichment factor from Wynn et al. (2010). Dissolved sulfate with an initial $\delta^{34}\text{S}$ value of 17.4‰ (derived from dissolution of primary sulfate from marine limestones, Fig. 3, a) is reduced by TSR, leaving remaining SO_4^{2-} increasingly ^{34}S -enriched by Rayleigh distillation (yellow path). The H_2S produced by TSR (red path) is initially ^{34}S -depleted (Fig. 3, b) by the isotope enrichment factor

$$\left(\varepsilon_{\text{TSR}}^{34} = \left[\left(\frac{^{34}\text{S}}{^{32}\text{S}} \right)_{\text{sulfate}} / \left(\frac{^{34}\text{S}}{^{32}\text{S}} \right)_{\text{sulfate}} - 1 \right] 1000\% \approx \delta_{\text{sulfate}} - \delta_{\text{sulfide}} \right)$$

the magnitude of $\varepsilon_{\text{TSR}}^{34}$ is T-dependent for TSR). As TSR reaction progress proceeds (moving to the left of the diagram) the reaction is either limited by the amount of electron donating hydrocarbons (e.g., methane in the Cerna Valley, Fig. 3, c) or by the amount of sulfate (Fig. 3, f). Both cases leave characteristic $\delta^{34}\text{S}$ values of coexisting dissolved S species, which are recognized in two groups of water chemistries in the aquifers of the Cerna region (Marin, 1984; Povařa et al., 2008; Wynn et al., 2010). The first group comprises the Northern Aquifer Complex, in which TSR is methane-limited, so the $\text{H}_2\text{S}:\text{SO}_4^{2-}$ ratio remains low. The resulting low $\delta^{34}\text{S}$ values of sulfide reflect the T-dependent enrichment factor between sulfide and sulfate (Fig. 3, c). The second group of water

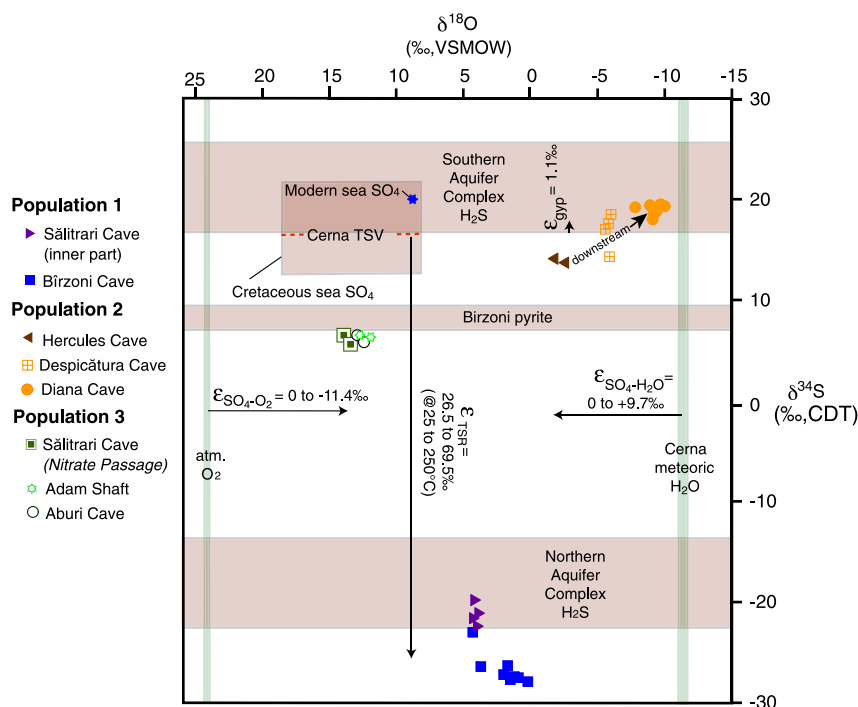


Fig. 2. Sulfur ($\delta^{34}\text{S}$) and oxygen ($\delta^{18}\text{O}$) isotope composition for cave sulfate minerals, in comparison to potential sources. The range of $\delta^{34}\text{S}$ values for pyrite from Birzoni cave is also plotted for reference, as are the ranges of $\delta^{34}\text{S}$ values for dissolved sulfide from the Northern and Southern Aquifer complexes, and mean value of total dissolved sulfur (TSV) of the Cerna Valley (from Wynn et al., 2010). Data for Cretaceous and modern seawater are from Turchyn et al. (2009), Claypool et al. (1980), and Holser et al. (1979), assuming $\epsilon^{18}_{\text{gypsum}}$ of $\sim 3.5\text{‰}$ and $\epsilon^{34}_{\text{gypsum}}$ of $\sim 1.1\text{‰}$. $\delta^{18}\text{O}$ values of atmospheric O_2 and meteoric water from the Cerna Valley are from Lloyd (1968) and Wynn et al. (2010), respectively. Sulfur and oxygen isotope enrichment factors (ϵ^{34} , ϵ^{18}) for TSR, sulfide oxidation to sulfate, and gypsum precipitation from sulfate is also shown for reference (values are T- and pathway-dependent).

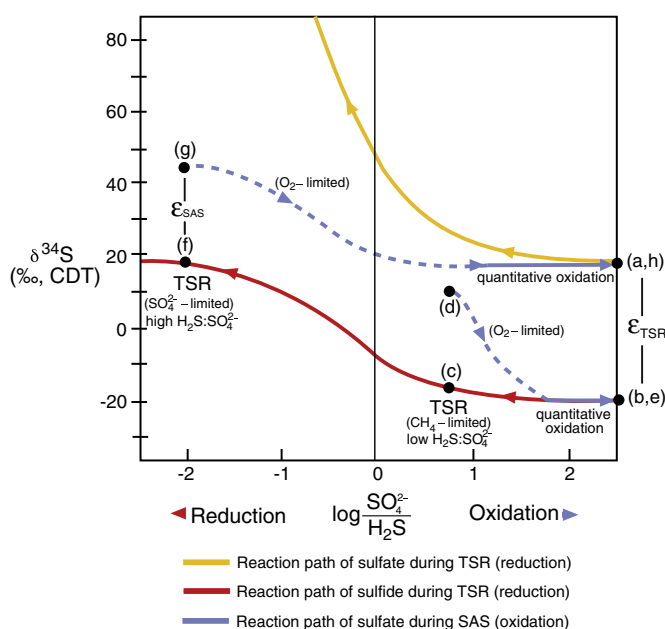


Fig. 3. Model of evolution of $\delta^{34}\text{S}$ values during TSR (reduction) and SAS (oxidation) in a closed system (modified from Ohmoto and Rye, 1979). Alpha labels denote specific points in the process relevant to the SAS in the Cerna Valley, and are discussed more thoroughly in the text. a) initial lithogenic source sulfate, b) initial sulfide produced by TSR, c) methane-limited sulfide produced by TSR (low $\text{H}_2\text{S}:\text{SO}_4^{2-}$ ratio), d) sulfate produced by oxidation of (c) under anoxic conditions, e) sulfate produced by oxidation of (c) under oxic conditions, f) sulfate-limited sulfide produced by TSR (high $\text{H}_2\text{S}:\text{SO}_4^{2-}$ ratio), g) sulfate produced by oxidation of (f) under anoxic conditions, h) sulfate produced by oxidation of (f) under oxic conditions.

chemistries comprises springs and wells downstream the intersection of the Cerna Syncline and Cerna Graben (Southern Aquifer Complex), below which point the waters have encountered high dissolved methane concentrations and geothermal heat, both of which drive the TSR reaction to completion ($\text{H}_2\text{S}:\text{SO}_4^{2-}$ ratios). Because these waters have relatively high concentrations of electron donors (methane), TSR is sulfate-limited, resulting in comparatively high $\text{H}_2\text{S}:\text{SO}_4^{2-}$ ratios. Such conditions produce dissolved sulfide with $\delta^{34}\text{S}$ values similar to those of the initial source sulfate (17.4‰, Fig. 3, f). An important caveat is that some of the waters chemistries are further modified by open-system conditions, and disproportion of intermediate S species may cause some further variation (Wynn et al., 2010).

These two endmembers of water chemistry provide initial conditions for the isotopic evolution of sulfate minerals produced by SAS (blue paths, reaction progress moves towards the right of Fig. 3). Because the fractionation factor during oxidation is generally small, initial sulfate produced by SAS has the $\delta^{34}\text{S}$ value of dissolved sulfide (plus any small fractionation factor during SAS ($\epsilon^{34}_{\text{SAS}}$ =

$$\left[\left(\frac{^{34}\text{S}}{^{32}\text{S}} \right)_{\text{sulfide}} / \left(\frac{^{34}\text{S}}{^{32}\text{S}} \right)_{\text{sulfate}} - 1 \right] 1000\text{‰} \approx \delta_{\text{sulfide}} - \delta_{\text{sulfate}}, \text{ Fig. 3 g}$$

and d). However, if the oxidation is quantitative, i.e. in oxic conditions, and no H_2S gas escapes, the sulfate produced by SAS takes on the $\delta^{34}\text{S}$ value of total dissolved sulfide (Fig. 3, h and e, solid blue paths). Thus, SAS results in $\delta^{34}\text{S}$ values of sulfate minerals that track the source of dissolved sulfide, as is generally the case with sulfide oxidation (Ohmoto, 1972; Ohmoto and Rye, 1979; Taylor and Wheeler, 1994). However, if oxidation is incomplete, i.e. anoxic conditions, the sulfate produced may take on intermediate $\delta^{34}\text{S}$ values, notably so if there is significant escape of H_2S gas, or other loss such as oxidation of H_2S by microbes or into base metal sulfides, or disproportionation of intermediate S species (Fig. 3 g and d, dashed blue paths).

Applying this model to the three endmember populations, we interpret the processes of S evolution during TSR and SAS; we later

validate and refine these interpretations using $\delta^{18}\text{O}$ values of the three populations.

Population 1 $\delta^{34}\text{S}$ values of these sulfates are consistent with oxidation of dissolved sulfide produced during methane-limited TSR (low $\text{H}_2\text{S}:\text{SO}_4^{2-}$) that characterizes the chemistry of springs in this area of the Northern Aquifer Complex (Wynn et al., 2010). In contrast, pyrites from the limestone bedrock in Bîrzoni cave have $\delta^{34}\text{S}$ values between +7.1‰ and +9.4‰ (Fig. 2). Such high values for pyrite are generally not characteristic of sedimentary pyrite produced by sulfate reducing bacteria where sulfate is abundant, as is typical of the sea floor (“open system” conditions; Canfield, 2001). Rather, these high $\delta^{34}\text{S}$ values are most parsimoniously attributed to a diagenetic origin, deriving from sulfate reduction in groundwater under sulfate-limited conditions (in an approximately “closed system” with respect to sulfate; Canfield, 2001). Irrespective of the source of this pyrite, acidic solutions resulting from its oxidation can not account for $\delta^{34}\text{S}$ values of the sulfates sampled in these caves.

Population 2 $\delta^{34}\text{S}$ values of these sulfates is compatible with oxidation of dissolved sulfide in springs of the Southern Aquifer Complex, which has $\delta^{34}\text{S}$ values characteristic of sulfate-limited, TSR (high $\text{H}_2\text{S}:\text{SO}_4^{2-}$). Here, dissolved sulfide has taken on the isotopic composition of initial dissolved sulfate before TSR (Wynn et al., 2010). Many of the springs in this Southern Aquifer Complex group show chemical compositions indicative of open system behavior with respect to reduced S species, which would tend to increase the $\delta^{34}\text{S}$ value of dissolved sulfide. This factor may contribute to $\delta^{34}\text{S}$ variation within this group, and we discuss this variation in more detail in light of $\delta^{18}\text{O}$ values of sulfate minerals below.

Population 3 Based solely on the intermediate $\delta^{34}\text{S}$ values of these sulfates, their formation may be consistent with two scenarios, and S isotopic composition does not uniquely identify the S source in this population. First, the $\delta^{34}\text{S}$ values of these cave sulfates are very similar to S isotopic composition of pyrite found in the limestone bedrock of Bîrzoni cave; as such they may derive from the oxidation of this diagenetic pyrite. Second, these intermediate $\delta^{34}\text{S}$ values may also be produced by oxidation of dissolved sulfide formed during methane-limited TSR, but with incomplete oxidation during SAS. We discuss these potential hypotheses below, in light of $\delta^{18}\text{O}$ values and considering two features which uniquely characterize the caves of this group. First, in Aburi Cave and Adam Shaft, large amounts of H_2S -rich steam outgas along a system of deep fractures. Second, ancient desiccated guano deposits, rich in speleogenetic by-products (alunite, aluminite, darapskite) overlie the siliciclastic sediment sequence in the Nitrate Passage of Sălitari Cave. Thus, it can be reasonably inferred that the Nitrate Passage was once a steam-heated environment (similar to Adam Shaft and Aburi Cave) in which oxidation of H_2S by atmospheric O_2 led to the acid-sulfate alteration and formation of gypsum, alunite, and other Al-sulfates with isotopic values in the same population as the other two steam caves (Fig. 2).

All $\delta^{34}\text{S}$ values of these sulfate minerals are consistent with oxidation of dissolved sulfide produced by TSR in the Cerna Valley geothermal field, with a Mesozoic marine limestone as the initial source of S involved in TSR. Given that there is currently no stratigraphic evidence of evaporite deposits in the shallow- and deep-water siliciclastic or carbonate rocks of the region (Năstăseanu, 1980), at least two line of

evidence independently support an initial marine source for sulfur involved in TSR: 1) the $\delta^{34}\text{S}$ values of total dissolved sulfur (TSV) in the region's thermo-mineral waters (Wynn et al., 2010) and 2) the high $\delta^{34}\text{S}$ value (8.1‰) of the diagenetic pyrite in limestone, which is difficult to explain without invoking a sulfate-limited, brackish to shallow marine environment (Berner and Raiswell, 1984; Bloch and Krouse, 1992).

6.2. O-isotope evolution during SAS: elucidation of sources of O

Because O in sulfate minerals is acquired during oxidation of sulfides, $\delta^{18}\text{O}$ values of sulfate can be informative of conditions present during SAS. Several factors are known to be important in controlling the O isotopic composition of sulfate minerals, providing constraints on their origins (Lloyd, 1968; Holser et al., 1979; Holt and Kumar, 1991; Taylor and Wheeler, 1994; Van Stempvoort and Krouse, 1994; Haubrich and Tichomirowa, 2002). These include: ambient conditions (pH, $p\text{O}_2$, T) and the type of sulfate-forming reactions (whether gas or aqueous phase) and resulting fractionation factors, as well as the amount and isotopic composition of O incorporated from two potential sources: (1) O_2 (either aqueous or gaseous, or potentially other oxidants such as NO_3^- , PO_4^{3-}) and (2) H_2O (either gas or liquid phase). Therefore, two fundamental limitations are provided by the $\delta^{18}\text{O}$ values of H_2O and of O_2 (see Reactions 1–3 above). With these constraints, $\delta^{18}\text{O}$ values of sulfate can be described by the equation:

$$\delta^{18}\text{O}_{\text{SO}_4^{2-}} = X(\delta^{18}\text{O}_{\text{H}_2\text{O}} + \varepsilon_{\text{SO}_4^{2-}-\text{H}_2\text{O}}^{18}) + (1-X)(\delta^{18}\text{O}_{\text{O}_2} + \varepsilon_{\text{SO}_4^{2-}-\text{O}_2}^{18})$$

where X is the fraction of O derived from water, ε the oxygen isotope enrichment factors between sulfate and water or oxygen:

$$\varepsilon_{\text{SO}_4^{2-}-y}^{18} = \left[\left(\frac{^{18}\text{O}/^{16}\text{O}}{\text{SO}_4} \right) / \left(\frac{^{18}\text{O}/^{16}\text{O}}{y} \right) - 1 \right] 1000 \approx \delta_{\text{SO}_4} - \delta_y, \text{ where}$$

y is either O_2 or H_2O . $\varepsilon_{\text{SO}_4^{2-}-\text{O}_2}^{18}$ varies significantly, but is always negative (0 to −11.4‰; can be near zero only when O_2 is stoichiometrically limited). Reported values for abiotic and biotic pathways are bound between −4.3 and −11.4‰, respectively (Van Stempvoort and Krouse, 1994 and references cited therein). $\varepsilon_{\text{SO}_4^{2-}-\text{H}_2\text{O}}^{18}$ also varies significantly, but is always positive (0 to +9.7‰), and varies predominantly as a function of oxidation rate and extent of sulfite-water exchange during intermediate oxidation steps (Van Stempvoort and Krouse, 1994 and references cited therein). Although the stoichiometric value of X represented in Reactions 1–3 is 0.25, sulfide oxidation occurs during several steps, and X can vary significantly depending on reaction conditions such as oxygen exchange between SO_3^{2-} (an intermediate product) and H_2O . Typical values are ~0.75 for saturated, anoxic conditions, but X can range from ~0 for “primary sulfate” to ~0.25 for oxic aqueous conditions to near 1 for abiotic reaction in saturated, anoxic conditions. Since we have no *a priori* knowledge of $\varepsilon_{\text{SO}_4^{2-}-y}^{18}$ values, we cannot quantitatively determine X, although we can qualitatively discriminate between the dominant O sources of the three populations of cave sulfates.

All cave sulfates $\delta^{18}\text{O}$ values from the Cerna Valley fall between the theoretical limitations outlined above ($\delta^{18}\text{O}_{\text{H}_2\text{O}} + \varepsilon_{\text{SO}_4^{2-}-\text{H}_2\text{O}}^{18}$ and $\delta^{18}\text{O}_{\text{O}_2} + \varepsilon_{\text{SO}_4^{2-}-\text{O}_2}^{18}$; Fig. 2, where $\delta^{18}\text{O}$ of local meteoric water is ~−11‰, Wynn et al., 2010, and that of atmospheric O_2 is +23.8‰; Horibe et al., 1973; note that equilibrium fractionation between dissolved and gaseous O_2 is comparatively small, ~−0.75‰; Benson et al., 1979). Sulfate minerals of Population 1 (Bîrzoni and Sălitari caves) suggest oxidation under more oxic conditions than those of Population 2 (Hercules, Despicațura and Diana caves), which showed $\delta^{34}\text{S}$ values indicating more complete, sulfate-limited TSR (high $\text{H}_2\text{S}:\text{SO}_4^{2-}$). The negative correlation between $\delta^{34}\text{S}$ and $\delta^{18}\text{O}$ values in the latter group of cave sulfates is consistent with increasing $\text{H}_2\text{S}:\text{SO}_4^{2-}$ ratios downstream (higher $\delta^{34}\text{S}$ values), and more anoxic conditions downstream (lower $\delta^{18}\text{O}$ values). This trend culminates in $\delta^{18}\text{O}$ values indicating near complete exclusion of O derived from O_2 in sulfate minerals from Diana

Cave. Thus, through the entire sequence of cave sulfates in the Cerna Valley, there is an increasing trend towards higher values of X downstream, confirming an increase in anoxic conditions of SAS in that direction. This is clearly consistent with the trend of increasingly complete TSR, higher $H_2S:SO_4^{2-}$ ratios, and greater anoxia in the same direction.

$\delta^{18}O$ values from the “steam caves” (Adam, Aburi, and presumably the Nitrate Passage of Săltirari Cave) are an outlier to this trend, and are indicative of the majority of sulfate O derived from atmospheric O_2 , with little incorporation of O derived from local meteoric water. The very high $\delta^{18}O$ values of these sulfates are consistent with “primary” sulfates as described by Holt and Kumar (1991), in which oxidation occurs prior to hydration. This process takes place in gas phase reactions during which ^{18}O is exchanged very abundantly with atmospheric $O_{2(g)}$, and negligibly with atmospheric $H_2O_{(g)}$. Since little or no equilibration occurs between sulfate and water during and after subsequent gypsum precipitation, these high-T sulfate minerals preserve the ^{18}O -enriched signature of the gas-phase oxidation reaction with nearly all O provided by O_2 .

6.3. S and O isotope evolution during SAS

The scenario we propose to explain S and O isotope variation in the caves of the Cerna Valley is described here in two distinct stages: TSR and SAS (Fig. 4). Regional groundwaters migrating towards the geothermal anomaly acquire the two reactants required for thermochemical sulfate reduction (TSR): dissolved sulfate and electron donors (in this case, predominantly methane). Meteoric-derived groundwater circulates through the Mesozoic sequence of karst rocks dissolving interstitial or bedded marine sulfates, which have a $\delta^{34}S$ value of about +17‰, producing total dissolved S concentrations that generally increase down-gradient. As these sulfate-bearing mineral waters

migrate along the Cerna Syncline towards the geothermal anomaly at Băile Herculane, they are heated and react with methane, which is likely produced from bacteriogenic processes in nearby coal deposits and migrates into the aquifers along faults transverse to the syncline. Although both the Northern and Southern Aquifer water chemistries provide reactants for TSR, divergent concentrations and redox conditions characterize each. Electron donors are present in low activity in the Northern Aquifer, but their activity is much higher in the Southern Aquifer, due to the presence of methane. This methane reduces large concentrations of dissolved SO_4^{2-} in waters of the Southern Aquifer Complex, giving these waters relatively high $H_2S:SO_4^{2-}$ ratios. Meanwhile, methane limits the extent of reduction in the Northern Aquifer Complex, so $H_2S:SO_4^{2-}$ ratios remain relatively low. These two pathways lead to diagnostic $\delta^{34}S$ and $\delta^{13}C$ values of dissolved sulfide and inorganic carbon (Fig. 4). The $\delta^{34}S$ signature of reduced S produced by TSR is later transferred to sulfate minerals during oxidation.

The TSR process described above provides the reduced S species that are the fuel for oxidative reactions which occur as anoxic groundwaters migrate upwards towards the oxic vadose zone, including many cave passages. Again, two distinct processes dominate in the Northern and Southern Aquifer systems, which differ largely in their oxidation potential (Fig. 4). Sulfide in the Northern Aquifer is oxidized by relatively abundant $O_{2(aq)}$, with most of the O in sulfate minerals ultimately derived from $O_{2(aq)}$, and the balance provided by $H_2O_{(l)}$. This reaction produces $\delta^{18}O$ values of sulfates minerals near those that would be predicted for hydration prior to oxidation and where all reactions attain equilibrium. Meanwhile in the Southern Aquifer complex, groundwaters are more anoxic due to more active TSR, and have relatively high $H_2S:SO_4^{2-}$ ratios. Here the oxidation of sulfide occurs in more anoxic conditions, which leaves $\delta^{18}O$ values of sulfate minerals near values that would be predicted for hydration occurring prior to complete oxidation. However, anoxic conditions of these waters lead to

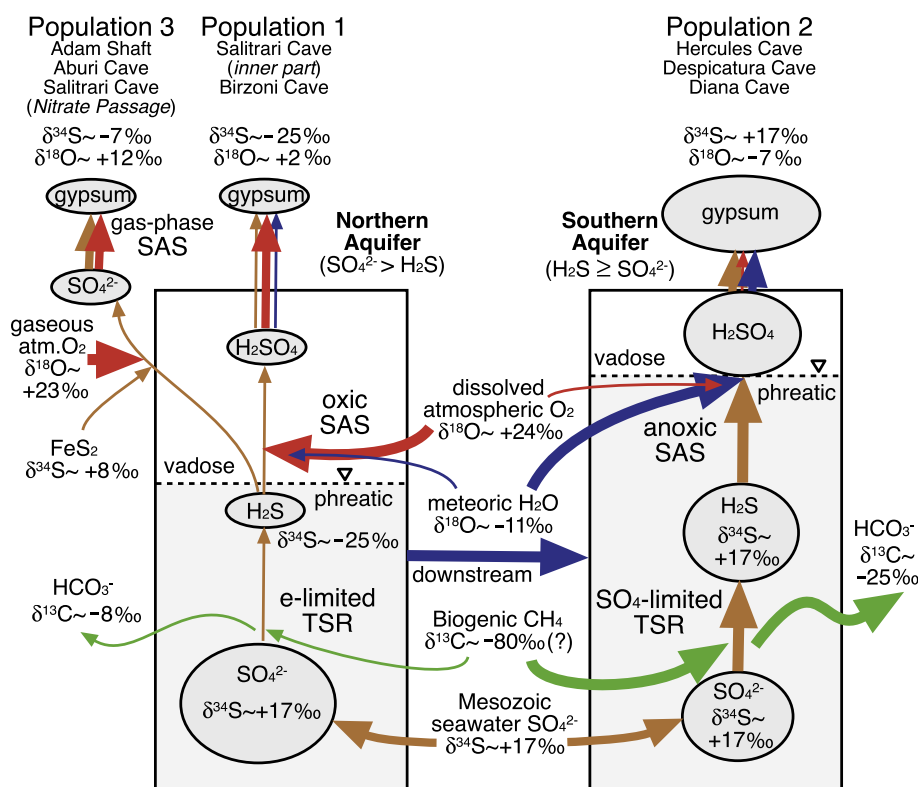


Fig. 4. Model of the processes leading to distinct populations of S and O isotopic composition in groundwaters and cave sulfate minerals (predominantly gypsum) in the Cerna Valley. Arrows representing fluxes of C, O, and S are color-coded by source (red = atmospheric O_2 , blue = meteoric H_2O , brown = Mesozoic SO_4^{2-} , and green = bacteriogenic CH_4). Arrow sizes are roughly proportional to fluxes.

abundant ^{18}O exchange with $\text{H}_2\text{O}_{(\text{l})}$ during hydration, and limited ^{18}O exchange with $\text{O}_{2(\text{aq})}$. Increasing contributions of O from $\text{H}_2\text{O}_{(\text{l})}$ -exchange are evident in increasingly anoxic conditions down-gradient (downstream in the Cerna Valley). A third population of sulfate minerals is found in association with steam caves. Here, the S is likely derived from methane-limited TSR, but some portion of dissolved sulfide may derive from pyrite that is found nearby, having intermediate signatures between the two endmembers. The oxygen isotopic composition of these sulfate minerals is unique in that there is no evidence of O derived from $\text{H}_2\text{O}_{(\text{g})}$ nor $\text{H}_2\text{O}_{(\text{l})}$; rather the $\delta^{18}\text{O}$ values are consistent with equilibrium oxidation of sulfides with O_2 in the gas phase, similar to “primary” sulfates in which sulfur is oxidized prior to hydration.

7. Conclusions and implications for SAS diagnoses

SAS has been shown in other karst regions of the world to produce sulfate deposits predominantly with ^{34}S -depleted isotopic signatures compared to their original sources of S in sulfate rocks. However, ^{34}S -depleted isotopic composition of the minerals alone does not provide enough information to clearly distinguish SAS from other more complex speleogenetic processes. Therefore it is important to note that complete studies investigating other parameters (concentrations of electron donors, initial isotopic composition of reservoirs, $\text{H}_2\text{S}:\text{SO}_4^{2-}$ ratios in groundwaters, etc.) are needed to precisely diagnose SAS. Caves in the Cerna region suggest strongly that SAS was the driving form of speleogenesis. Whether the main SAS phase occurred at or near the water table or deeper in the karst system is still debatable and important for understanding carbonate dissolution and sulfate precipitation mechanisms.

Sulfate mineral $\delta^{34}\text{S}$ values in the Cerna region show that cave sulfate isotope values from SAS depend not only on the source of the S, but also on the completeness of subsequent S species reactions. This study has demonstrated that in a single hydrological system, this variation produces a relatively wide range of $\delta^{34}\text{S}$ values (from -27.9 to $+19.2\text{‰}$). A study of the S isotopic composition of the thermo-mineral waters (Wynn et al., 2010), showed that relatively variable concentrations of an electron donor (methane) coupled with increasing concentrations of total dissolved S, drives differences in the extent of sulfate reduction, allowing for the progression of sulfate reduction to be seen in the waters of the wells and springs of the Cerna region. Other aquifers and systems where SAS occurs tend to have large sulfate sources compared to the concentration of electron donors, resulting in partial, or incomplete reduction, accompanied by large fractionation factors (i.e., electron donors are consumed before the reservoir of sulfate significantly changes isotopic composition). The correspondence between the sulfur isotopic composition of sulfate minerals in the Cerna Valley and that of dissolved S species in the Cerna aquifer waters clearly indicates that cave minerals are produced from these reservoirs.

The importance of this study lies, in part, in its description of a unique mineralogical and geochemical setting that provides important information on the S cycle in the region and the processes and conditions occurring in caves along the Cerna Valley that can be applied elsewhere. It also provides an approach for the identification and interpretation of multiple and temporally disparate events of speleogenesis that may not be uniquely preserved as diagnostic morphologic features or mineral assemblages. As such, the integration of cave mineralogy and morphology studies with broad hydrogeochemical data used in this study serves as an example of how we may more completely recognize additional processes and parameters that may be involved in SAS.

The ability to reliably document different cave sulfate populations is critical to understanding of S sources, hydrological and speleogenetic processes, and to quantifying the role of thermo-mineral waters on mineral deposition and cave morphology. In addition, the presence of large guano deposits can play an important role and provide a

geochemical system that produces sulfate deposits with varying isotopic compositions. Finally, the use of oxygen- and sulfur-isotope systematics of sulfate minerals precipitated in a variety of cave settings may also shed light on similar processes occurring during emplacement of ore deposits or in acid sulfate alteration environments. For example, given the present understanding of the oxygen isotopic composition of sulfate, the oxygen isotope fractionation between sulfate and OH^- in some sulfates (mainly alunite) may now be used as a geothermometer for alunite formation (Rye, 2005). Such studies are valuable in deciphering the source of fluids, degree of mixing, regional groundwater dynamics, and other hydrogeochemical processes.

Acknowledgments

We thank the Domogled-Valea Cernei National Park for logistic support to conduct our research. Dr. Ioan Povară from the “Emil Racoviță” Institute of Speleology and Lucian Nicolici (Prusik Timișoara Speleo Club) provided an indispensable assistance during our field campaigns. The paper was improved by helpful comments provided by Editor U. Brand and two anonymous reviewers. The Romanian National University Research Council (grant ID_544 to Onac) contributed funds for this research.

References

- Angert, E.R., Northup, D.E., Reysenbach, A.L., Peek, A.S., Goebel, B.M., Pace, N.R., 1998. Molecular phylogenetic analysis of a bacterial community in Sulphur River, Parker Cave, Kentucky. *American Mineralogist* 83, 1583–1592.
- Audra, P., Hoblea, F., Bigot, J.Y., Nobecourt, J.-C., 2007. The role of condensation corrosion in thermal speleogenesis: study of a hypogenic sulfidic cave in Aix-les-Bains, France. *Acta Carsologica* 36, 185–194.
- Barton, H.A., Northup, D.E., 2007. Geomicrobiology in cave environments: past, current and future perspectives. *Journal of Cave and Karst Studies* 69, 163–178.
- Benson, B.B., Krause Jr., D., Peterson, M.A., 1979. The solubility and isotopic fractionation of gases in dilute aquatic solution. I. Oxygen. *Journal of Solution Chemistry* 8, 655–690.
- Bercia, E., Năstăseanu, S., Berza, T., Iancu, V., Stănoiu, I., Hirtopanu, I., 1987. Obirșia Cloșani Sheet, 1:50,000, Institutul de Geologie și Geofizică, București.
- Berner, R.A., Raiswell, R., 1984. C/S method for distinguishing freshwater from marine sedimentary rocks. *Geology* 12, 365–368.
- Bloch, J., Krouse, H.R., 1992. Sulfide diagenesis and sedimentation in the Albian Herman Member, Western Canada. *Journal of Sedimentary Petrology* 62, 235–249.
- Bottrell, S.H., 1991. Sulphur isotope evidence for the origin of cave evaporites at Ogof y Daren Cilau, south Wales. *Mineralogical Magazine* 55, 209–210.
- Bottrell, S.H., Newton, R.J., 2006. Reconstruction of changes in global sulfur cycling from marine sulfate isotopes. *Earth Science Reviews* 75, 59–83.
- Bottrell, S.H., Carew, J.L., Mylroie, J.E., 1993. Inorganic and bacteriogenic origins for sulfate crusts in flank margin caves, San Salvador Island, Bahamas. *Proceedings of the 6th Symposium on the Geology of the Bahamas*, pp. 17–21.
- Bottrell, S.H., Crowley, S., Self, C., 2001. Invasion of a karst aquifer by hydrothermal fluids: evidence from stable isotopic compositions of cave mineralization. *Geofluids* 1, 103–121.
- Canfield, D.E., 2001. Biogeochemistry of sulfur isotopes. *Reviews in Mineralogy and Geochemistry* 43, 607–636.
- Canfield, D.E., 2004. The evolution of the Earth surface sulfur reservoir. *American Journal of Science* 304, 839–861.
- Claypool, G.E., Holser, W.T., Kaplan, I.R., Sakai, H., Zak, I., 1980. The age curves of sulfur and oxygen isotopes in marine sulfate and their mutual interpretation. *Chemical Geology* 28, 199–260.
- Cristescu, I., 1978. Tezaurul Cernei (Cerna's Treasure). Ed. Sport-Turism, București, 176 pp.
- Demetrescu, C., Andreescu, M., 1994. On the thermal regime of some tectonic units in a continental collision environment in Romania. *Tectonophysics* 230, 265–276.
- DuChene, H.R., 1997. Lechuguilla Cave, New Mexico, U.S.A. In: Hill, C.A., Forti, P. (Eds.), *Cave Minerals of the World*, second ed. National Speleological Society, Huntsville, Alabama, pp. 343–350.
- Engel, A.S., Stern, L.A., Bennett, P.C., 2004. Microbial contributions to cave formation: new insights into sulfuric acid speleogenesis. *Geology* 32 (5), 369–372.
- Egemeier, S.J., 1973. Cavern development by thermal waters with a possible bearing on ore deposits. Unpublished PhD thesis, Stanford University, 88 pp.
- Fry, B., Ruf, W., Gest, H., Hayes, J.M., 1988. Sulfur isotope effects associated with oxidation of sulfide by O_2 in aqueous solution. *Chemical Geology* 73, 205–210.
- Galdenzi, S., Menichetti, M., 1995. Occurrence of hypogenic caves in a karst region: examples from central Italy. *Environmental Geology* 26, 39–47.
- Galdenzi, S., Maruoka, T., 2003. Gypsum deposits in the Frasassi Caves, central Italy. *Journal of Cave and Karst Studies* 65, 111–125.
- Gheorghe, A., Crăciun, P., 1993. Thermal aquifers in Romania. *Journal of Hydrology* 145, 111–123.

- Grasby, S.E., van Everdingen, R.O., Bednarski, J., Lepitzki, D.A.W., 2003. Travertine mounds of the Cave and Basin National Historic Site, Banff National Park. *Canadian Journal of Earth Sciences* 40, 1501–1513.
- Grassineau, N., Matthey, D., Lowry, D., 2001. Sulfur isotope analysis of sulfide and sulfate minerals by continuous flow-isotope ratio mass spectrometry. *Analytical Chemistry* 73, 220–225.
- Haubrich, F., Tichomirowa, M., 2002. Sulfur and oxygen isotope geochemistry of acid mine drainage — the polymetallic sulfide deposit “Himmelfahrt Fundgrube” in Freiburg, Germany. *Isotopes in Environmental and Health Studies* 38, 121–138.
- Hill, C.A., 1981. Speleogenesis of Carlsbad caverns and other caves of the Guadalupe Mountains. *Proceedings of the 8th International Congress of Speleology*, Bowling Green, pp. 143–144.
- Hill, C.A., 1987. Speleogenesis of Carlsbad Caverns and other caves in the Guadalupe Mountains, New Mexico and Texas. *New Mexico Bureau of Mines and Mineral Resources Bulletin* 117 (150 pp.).
- Hill, C.A., 1990. Sulfuric acid speleogenesis of Carlsbad Cavern and its relationship to hydrocarbons, Delaware Basin, New Mexico and Texas. *American Association of Petroleum Geologists Bulletin* 74, 1685–1694.
- Hill, C.A., 1995. Sulfur redox reactions: hydrocarbons, native sulfur, Mississippi Valley-type deposits, and sulfuric acid karst in the Delaware Basin, New Mexico and Texas. *Environmental Geology* 25, 16–23.
- Hill, C.A., Forti, P., 1997. Cave minerals of the world, second ed. National Speleological Society, Huntsville, Alabama. 463 pp.
- Holser, W.T., Kaplan, I.R., Sakai, H., Zak, I., 1979. Isotope geochemistry of oxygen in the sedimentary sulfate cycle. *Chemical Geology* 25, 1–17.
- Holt, B.D., Kumar, R., 1991. Oxygen isotope fractionation for understanding the sulphur cycle. In: Krouse, H.R., Grinenko, V.A. (Eds.), *Stable Isotopes in the Assessment of Natural and Anthropogenic Sulphur in the Environment*. Wiley & Sons, New York, pp. 27–41.
- Horibe, Y., Shigehara, K., Takakuwa, Y., 1973. Isotope separation factors of carbon dioxide-water system and isotopic composition of atmospheric oxygen. *Journal of Geophysical Research* 78, 2625–2629.
- Hoefs, J., 2009. *Stable isotope geochemistry*, sixth ed. Springer, New York. (244 pp.).
- Hose, L.D., Palmer, A.N., Palmer, M.V., Northup, D.E., Boston, P.J., DuChene, H.R., 2000. Microbiology and geochemistry in a hydrogen sulphide rich karst environment. *Chemical Geology* 169, 399–423.
- Iancu, V., Berza, T., Szeghedi, A., Marunțiu, M., 2005. Palaeozoic rock assemblages incorporated in the South Carpathian Alpine thrust belt (Romania and Serbia): a review. *Geologica Belgica* 8, 48–68.
- Jagnow, D.H., 1977. Geologic factors influencing speleogenesis in the Capitan reef complex, New Mexico and Texas [MS thesis], University of New Mexico, 203 pp.
- Jagnow, D.H., Hill, C.A., Davis, D.G., DuChene, H.R., Cunningham, K.I., Northup, D.E., Queen, J.M., 2000. History of the sulfuric acid theory of speleogenesis in the Guadalupe Mountains, New Mexico. *Journal of Cave and Karst Studies* 62, 54–59.
- Kaplan, I.R., Rittenberg, S.C., 1964. Microbiological fractionation of sulphur isotopes. *Journal of General Microbiology* 34, 195–212.
- Klimchouk, A.B., 2007. Hypogene speleogenesis: hydrogeologic and morphogenetic perspective. National Cave and Karst Research Institute Special Publication, 1 (106 pp.).
- Liégeois, J.P., Berza, T., Tatu, M., Duchesne, J.C., 1996. The Neoproterozoic Pan-African basement from the Alpine lower Danubian nappe system (South Carpathians, Romania). *Precambrian Research* 80, 281–301.
- Lloyd, R.M., 1968. Oxygen isotope behavior in the sulfate-water system. *Journal of Geophysical Research* 73, 6099–6110.
- Lueth, V.W., Rye, R.O., Peters, L., 2005. “Sour gas” hydrothermal jarosite: ancient to modern acid sulfate mineralization in the southern Rio Grande Rift. *Chemical Geology* 215, 339–360.
- Macalady, J.L., Lyon, E.H., Koffman, B., Albertson, L.K., Meyer, K., Galdenzi, S., Mariani, S., 2006. Dominant microbial populations in limestone-corroding stream biofilms, Frasassi cave system, Italy. *Applied and Environmental Microbiology* 72 (8), 5596–5609.
- Mandeville, C.W., 2010. Sulfur: a ubiquitous and useful tracer in earth and planetary sciences. *Elements* 6, 75–80.
- Marin, C., 1984. Hydrochemical considerations in the lower Cerna river basin. *Theoretical and Applied Karstology* 1, 173–183.
- Morehouse, D.F., 1968. Cave development via the sulfuric acid reaction. *National Speleological Society Bulletin* 30 (1), 1–10.
- Năstăseanu, S., 1980. *Géologie des Monts Cerna*. Anuarul Institutului de Geologie și Geofizică LIV. (137 pp.).
- Nehring, N.L., Bowen, P.A., Truesdell, A.H., 1977. Technique for the conversion to carbon dioxide of oxygen from dissolved sulfate in thermal waters. *Geothermics* 5, 63–66.
- Ohmoto, H., 1972. Systematics of sulfur and carbon isotopes in hydrothermal ore deposits. *Economic Geology* 67, 551–578.
- Ohmoto, H., Rye, R.O., 1979. Isotopes of sulfur and carbon. In: Barnes, H.L. (Ed.), *Geochemistry of Hydrothermal Ore Deposits*, second ed. John Wiley & Sons, pp. 509–567.
- Onac, B.P., 2005. Minerals. In: Culver, D.C., White, W.B. (Eds.), *Encyclopedia of Caves*. Academic Press, New York, pp. 371–378.
- Onac, B.P., Forti, P., 2011. State of the art and challenges in cave minerals studies. *Studia UBB Geologia* 56 (1), 33–42.
- Onac, B.P., Hess, J.W., White, W.B., 2007. The relationship between the mineralization of breccia pipes and mineral composition of speleothems: evidence from Corkscrew Cave, Arizona, USA. *Canadian Mineralogist* 45, 1177–1188.
- Onac, B.P., Sumrall, J., Tămaș, T., Povară, I., Kearns, J., Dărmiceanu, V., Vereș, D., Lascu, C., 2009. The relationship between cave minerals and H₂S-rich thermal waters along the Cerna Valley (SW Romania). *Acta Carsologica* 38, 67–79.
- Ono, S., 2008. Multiple-sulphur isotope biosignatures. *Space Science Reviews* 135, 203–220.
- Palmer, A.N., 2007. *Cave Geology*. Cave Books, Dayton, OH. 454 pp.
- Palmer, A.N., Hill, C.A., 2005. Sulfuric acid caves. In: Culver, D.C., White, W.B. (Eds.), *Encyclopedia of Caves*. Academic Press, New York, pp. 573–581.
- Pisarowicz, J.A., 1994. Cueva de Villa Luz — an active case of H₂S speleogenesis. In: Sasowsky, I.D., Palmer, M.V. (Eds.), *Breakthroughs in Karst Geomicrobiology*. Colorado Springs, Colorado, pp. 60–62.
- Polyak, V.J., Provencio, P., 2001. By-product materials related to H₂S–H₂SO₄ influenced speleogenesis of Carlsbad, Lechuguilla, and other caves of the Guadalupe Mountains, New Mexico. *Journal of Cave and Karst Studies* 63, 23–32.
- Polyak, V.J., McIntosh, W.C., Güven, N., Provencio, P., 1998. Age and origin of Carlsbad Cavern and related caves from ⁴⁰Ar/³⁹Ar of alunite. *Science* 279, 1919–1922.
- Povară, I., 2001. Thermal springs in Baile Herculane (Romania). In: LaMoreaux, P.E., Tanner, J.T. (Eds.), *Spring and Bottled Waters of the World: Ancient history, Source, Occurrence, Quality, and Use*. Springer, pp. 210–216.
- Povară, I., Diaconu, G., Goran, C., 1972. Observations préliminaires sur les grottes influencées par les eaux thermo-minérales de la zone Baile-Herculane. *Travaux de l'Institut de Spéologie "Emile Racovitz"*, XI: 355–365.
- Povară, I., Simion, G., Marin, M., 2008. Thermomineral waters from the Cerna Valley Basin (Romania). *Studia UBB, Geologia* 53, 41–54.
- Puşcaş, C., Onac, B., Tămaș, T., 2010. The mineral assemblage of caves within Şalitrari Mountain (Cerna Valley, SW Romania): depositional environment and speleogenetic implications. *Carbonates and Evaporites* 25 (2), 107–115.
- Rye, R.O., 2005. A review of the stable-isotope geochemistry of sulfate minerals in selected igneous environments and related hydrothermal systems. *Chemical Geology* 215, 5–36.
- Sarbu, S.M., Kane, T.C., Kinkle, B.K., 1996. A chemoautotrophically based cave ecosystem. *Science* 272, 1953–1955.
- Seal II, R.R., Rye, R.O., Alpers, C.N., 2000. Stable isotope systematics of sulfate minerals. *Reviews in Mineralogy and Geochemistry* 40, 541–602.
- Schoen, R., Rye, R.O., 1970. Sulfur isotope distribution in solfataras, Yellowstone National Park. *Science* 170, 1082–1084.
- Spirakis, C., Cunningham, K.I., 1992. Genesis of sulfur deposits in Lechuguilla Cave, Carlsbad Caverns National Park, New Mexico. In: Wessel, G., Kimberley, B. (Eds.), *Native Sulfur — Developments in Geology and Exploration*, American Institute of Mining, Metallurgical, and Petroleum Engineers (AIME), pp. 139–145.
- Swezey, C.S., Piatak, N.M., Chiehowsky, L.A., Hadden, R.L., Hackley, P.C., Doolan, C.A., Aleman Gonzalez, W.B., Bingham, P.A., Hoke, R.B., 2004. A guide to the geology of the Sinnott-Thorn Mountain cave system, Pendleton County, West Virginia. *The Potomac Caver* 47, 3–14.
- Taylor, B., Wheeler, M., 1994. Sulfur- and oxygen- isotope geochemistry of acid mine drainage in the western United States: field and experimental studies revisited. In: Alpers, C., Blowes, D. (Eds.), *Environmental Geochemistry of Sulfide Oxidation*. American Chemical Society Symposium Series, 550, pp. 481–514.
- Turchyn, A.V., Schrag, D.P., Coccioni, R., Montanari, A., 2009. Stable isotope analysis of the Cretaceous sulfur cycle. *Earth and Planetary Science Letters* 285, 115–123.
- van Everdingen, R.O., Shakur, M.A., Krouse, H.R., 1985. Role of corrosion by H₂SO₄ fallout in cave development in a travertine deposit — evidence from sulfur and oxygen isotopes. *Chemical Geology* 49, 205–211.
- Veliciu, S., 1998. Contributions to the geothermic investigation of the thermal waters with applications to R. S. Romania. *Studii Tehnice și Economice, Seria D. Geofizica* 15 (in Romanian).
- Van Stempvoort, D.R., Krouse, H.R., 1994. Controls of sulfate δ¹⁸O: a general model and application to specific environments. In: Alpers, C., Blowes, D. (Eds.), *Environmental Geochemistry of Sulfide Oxidation*. American Chemical Society Symposium Series, 550, pp. 446–480.
- Vlasceanu, L., Sarbu, S.M., Engel, A.S., Kinkle, B.K., 2000. Acidic, cave-wall biofilms located in the Frasassi Gorge, Italy. *Geomicrobiology Journal* 17, 125–139.
- Wynn, J.G., Sumrall, J.B., Onac, B.P., 2010. Sulfur isotopic composition and the source of dissolved sulfur species in thermo-mineral springs of the Cerna Valley, Romania. *Chemical Geology* 271, 31–43.
- Yonge, C.J., Krouse, H.R., 1987. The origin of sulfates in Castleguard cave, Columbia Icefields Canada. *Chemical Geology* 65, 427–433.
- Zhang, J.Z., Millero, F.J., 1994. Kinetics of oxidation of hydrogen-sulfide in natural waters. In: Alpers, C., Blowes, D. (Eds.), *Environmental Geochemistry of Sulfide Oxidation*. American Chemical Society Symposium Series, 550, pp. 393–409.